

# Soft solution fluorine-free synthesis of anatase nanoparticles with tailored morphology

David G. Calatayud<sup>a,\*</sup>, Teresa Jardiel<sup>a</sup>, Mónica Rodríguez<sup>a</sup>, Marco Peiteado<sup>a,b</sup>,  
Daniel Fernández-Hevia<sup>c,d</sup>, Amador C. Caballero<sup>a</sup>

<sup>a</sup>Department of Electroceramics, Instituto de Cerámica y Vidrio, CSIC, c/Kelsen 5, Campus de Cantoblanco, 28049 Madrid, Spain

<sup>b</sup>Department of Applied Physics, ETSI Telecomunicación, UPM, Avda. de la Complutense, 28040 Madrid, Spain

<sup>c</sup>INAEI Electrical Systems, S.A. c/Jarama 5, 45007 Toledo, Spain

<sup>d</sup>Department of Chemistry, Universidad de Las Palmas de Gran Canaria, Campus de Tafira, E-35017 Gran Canaria, Spain

Received 4 June 2012; received in revised form 12 July 2012; accepted 13 July 2012

Available online 20 July 2012

## Abstract

TiO<sub>2</sub> nanoparticles with tailored morphology have been synthesized under exceptionally soft conditions. The strategy is based on the use of a non-aqueous alcoholic reaction medium in which water traces, coming either from the air (atmospheric water) or from an ethanol–water azeotropic mixture (ethanol 96%), are incorporated in order to accelerate hydrolysis of the Ti–precursor. Moreover, organic surfactants have been used as capping agents so as to tailor crystal growth in certain preferential directions. Combinations of oleic acid and oleylamine, which lead to the formation of another surfactant, dioleamide, are employed instead of fluorine-based compounds, thus increasing the sustainability of the process. As a result, TiO<sub>2</sub> nanostructured hierarchical microspheres and individual nanoparticles with exposed high-energy facets can be obtained at atmospheric pressure and temperatures as low as 78 °C.

© 2012 Elsevier Ltd and Techna Group S.r.l. All rights reserved.

**Keywords:** A. Powders: chemical preparation; A. Grain growth; B. Electron microscopy; D. TiO<sub>2</sub> anatase

## 1. Introduction

In recent years the number of published works dealing with obtaining TiO<sub>2</sub> nanoparticles with ultra-reactive surfaces has increased exponentially, mainly due to the great interest in their high reactivity that arises both from a scientific and technological point of view. The unique physicochemical properties of TiO<sub>2</sub> nanoparticles confer them with potential applications in a wide range of fields, acting as photocatalysts, dye-sensitive solar cells (DSCs), Li batteries, transparent conductors, gas sensors, and so on [1–13]. These properties depend not only on the crystal phase, particle size and distribution of the particles, but also on their specific morphology, since the latter can lead to a reduction in the formation of electron traps and thus facilitate the electron transfer in the semiconductor

structure [1,2,14–19]. In particular, for photocatalytic applications materials based on high-energy faceted anatase nanocrystals or, as recently reported, on crystalline hierarchical TiO<sub>2</sub> hollow spheres [20–22] are required, in order to achieve a high efficiency. Accordingly, the synthesis of well-crystallized and nanostructured TiO<sub>2</sub> particles with tailored morphology represents a major challenge.

The formation and growth of TiO<sub>2</sub> nanoparticles is generally achieved through hydrolysis and condensation processes from different precursors. The major problem tailoring the morphology and size of these particles arises from the titanium ions themselves: Ti<sup>4+</sup> cations are large and highly electropositive, and therefore prone to suffer a nucleophilic attack by water, which leads to a too fast hydrolysis and thus to uncontrolled growths and precipitations. One of the most effective ways to control the rate of hydrolysis is through the choice of the metal alkoxide, e.g. altering the OR groups. The alkoxy groups which are most frequently used in the synthesis of TiO<sub>2</sub> comprise from 2 (ethoxide) to 4 (butoxide) carbon atoms, and their

\*Corresponding author. Tel.: +34 917355840x1184;  
fax: +34 917355843.

E-mail address: [dgcalatayud@icv.csic.es](mailto:dgcalatayud@icv.csic.es) (D.G. Calatayud).

reactivity during the hydrolysis decreases with increasing chain length. However, in the presence of excess of water, hydrolysis is still exothermic and quick and completed in seconds. A feasible way of further reducing this speed is by adjusting the  $H_2O/M(OR)_n$  ratio and stabilizing the formed colloids. What is more, the replacement of the alkoxy groups by less hydrolyzable ones may also contribute to decrease the rates of hydrolysis and condensation, affecting the crystallization behavior and increasing the control over the final particle size. Even with these procedures, the overall hydrolysis reaction of  $Ti^{4+}$  ions still remains too fast, and thus a very fine control of the reaction conditions is a necessary requirement, since any slight alteration of the reaction kinetics will cause dramatic changes in the size and morphology of the final material.

In order to overcome this drawback, non-hydrolytic processes have been described for obtaining  $TiO_2$  nanoparticles with high crystallinity. The use of oxygen donor groups other than water may allow a better control of the reaction rate, leading to slow particle growth. The problem is that under these conditions the reaction rate is drastically reduced, the process becomes excessively slow and the possibility of tailoring the morphology of the synthesized particles is hindered by kinetic considerations [23–27]. In this sense a promising alternative which has been recently considered combines both hydrolytic and non-hydrolytic reactions: by adding a certain amount of water into a non-aqueous media, the size and morphology of the  $TiO_2$  precipitated particles can be finely tuned [28].

However, for the particular case of high-energy faceted  $TiO_2$  nanocrystals an extra problem needs to be faced: due to minimization of the surface energy, the number of highly reactive faces rapidly decreases during the crystallization process. This means that under normal conditions the synthesized  $TiO_2$  crystals consist mainly of poorly reactive  $\{101\}$  faces, which are thermodynamically more stable than the desired  $\{001\}$  and  $\{010\}$  faces (Fig. 1). In order to reverse this situation, i.e. to stabilize the more reactive faces, a characteristic resource is the use of morphological agents that cap the growth in one or more

faces, making the crystal develop only in certain directions and hence altering/controlling its morphology [29]. Hydrofluoric acid is one of these agents, and different experimental and theoretical studies have proved its efficiency producing faceted  $TiO_2$  crystals with high percentages of  $\{001\}$  and  $\{010\}$  faces [30–33]. Most recent works on the synthesis of faceted  $TiO_2$  follow this methodology, in which fluorine anions selectively adsorb on the surface of  $\{010\}$  and  $\{001\}$  faces, stabilizing them. However, the use of fluorinated compounds as morphological control agents also carries some disadvantages: first an input of pressure and temperatures around  $180\text{ }^\circ\text{C}$  are typically required so as to obtain the properly crystallized faceted particles. Moreover, during the reaction process a release of highly corrosive hydrofluoric vapors is always observed, which undoubtedly represents a major drawback for the large-scale synthesis of faceted  $TiO_2$ . In view of these facts, the substitution of fluorine-based compounds by organic capping surfactants which usually contain amine, amide or carboxylic groups, must be considered. Used either individually or combined [25–28,34–36], these molecules represent a more environmentally-friendly option to tune the morphology of the anatase particles. To be more precise, Dinh et al. [28] have recently proved different combinations of oleic acid and oleylamine to successfully synthesize  $TiO_2$  crystals with different shapes. The problem with fluorine vapors is consequently eradicated when using this method, but temperatures around  $180\text{ }^\circ\text{C}$  and the use of a sealed autoclave reactor to autogenously increase the pressure are still required.

In this sense, herein we report a new synthetic approach based on a non-aqueous and fluorine-free technique to obtain  $TiO_2$  nanocrystals with tailored morphology at atmospheric pressure and temperature clearly below  $100\text{ }^\circ\text{C}$ . Nanostructured hierarchical  $TiO_2$  spheres as well as individual faceted anatase nanocrystals are successfully prepared at remarkably soft conditions. Oleic acid and oleylamine are combined and used as morphological control agents, and their capping role is analyzed and reinterpreted in terms of the formation of the dioleamide as a surfactant molecule.

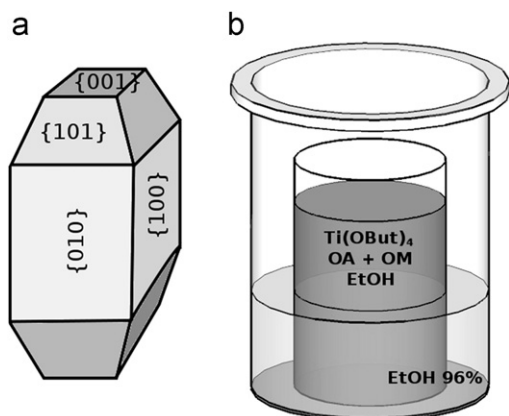


Fig. 1. (a) Anatase  $TiO_2$  with  $\{101\}$ ,  $\{001\}$  and  $\{010\}/\{100\}$  facets and (b) scheme of the reaction assembly for the nanoparticles synthesis.

## 2. Materials and methods

### 2.1. Chemicals

The chemicals titanium (IV) tetrabutoxide ( $Ti(OBu)_4$ , Fluka, 98%), ethanol (EtOH, Merck, analytically pure), oleic acid ((Z)-octadec-9-enoic acid, designated as OA, Fluka, analytically pure), and oleylamine ((Z)-octadec-9-en-1-amine, designated as OM, Aldrich, 70%) were used without further purification.

### 2.2. Synthesis of $TiO_2$ spheres (TiS)

A solution of  $Ti(OBu)_4$  (10 mmol) in 200 mL of dry ethanol was stirred under reflux for 8 h. Then the solution

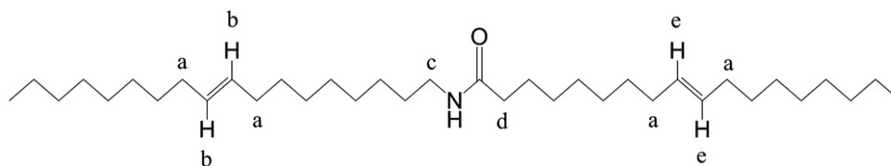


Fig. 2. Dioleamide (DO).

was evaporated to dryness, and the obtained white solid was washed with deionized water and dried at room temperature. The as-synthesized  $\text{TiO}_2$  spheres were calcined at 300 and 400 °C for 4 h so as to remove organic products and promote crystallinity.

### 2.3. Synthesis of dioleamide (DO)

OA (3.55 g, 12.5 mmol) and OM (70%, 4.80 g, 12.5 mmol) were mixed in a flask under stirring, heat release was appreciated. The obtained yellow liquid was dried with  $\text{MgSO}_4$ . Yield: 99%.  $^1\text{H}$  NMR (300 MHz,  $\text{DMSO-d}_6$ ,  $\delta$ ): 7.35 (s, 2H,  $\text{H}_b$ ), 5.28 (m, 3H,  $\text{H}_c + \text{NH}$ ), 2.66 (s, 2H,  $\text{H}_c$ ), 1.98 (s, 8H,  $\text{H}_a$ ), 1.51 (s, 2H,  $\text{H}_d$ ), 1.26 (s, 46H,  $\text{CH}_2$ ), 0.85 (q, 6H,  $\text{CH}_3$ ) (see Fig. 2).

### 2.4. Synthesis of $\text{TiO}_2$ nanoparticles (TiNP)

In a typical procedure,  $\text{Ti}(\text{OBut})_4$  (10 mmol) was added to a mixture of X mmol OA, Y mmol OM, in 5:5 or 6:4 ratios, and 200 mmol of dry ethanol. The Pyrex beaker containing the obtained mixture was placed into an automated laboratory reactor system (Mettler-Toledo LabMax) containing 80 mL of ethanol 96% (see Fig. 1). Then the reaction was heated under stirring at 78 °C for 8 h or 72 h. The obtained precipitate was washed with dry ethanol and deionized water several times and then dried at room temperature.

### 2.5. Surface surfactants removal from as-prepared anatase TiNP

Solid samples of the as-prepared anatase  $\text{TiO}_2$  nanoparticles were heated at 200 °C for 30 min. The obtained orange solids were then washed with hot dry ethanol under stirring several times. Finally the obtained white precipitates were washed with deionized water and one last time with ethanol. The clean samples were dried at 80 °C in air.

### 2.6. Characterization

The analyses of the crystalline structure and phase identification were performed by X-ray diffraction (XRD Bruker D8 ADVANCE) with a monochromatized source of  $\text{CuK}_{\alpha 1}$  radiation ( $\lambda = 1.5406$  nm) at 1.6 kW (40 kV, 40 mA). Samples were prepared by placing a drop of a concentrated ethanolic dispersion of particles onto a silicon single crystal. FESEM images were obtained with a Hitachi S-4700 field-emission scanning electron

microscope (FESEM) working at 20 kV. Transmission electron microscopy (TEM) images were collected in a HITACHI H7100 microscope working at 125 kV and high-resolution transmission electron microscopy (HRTEM) images were obtained on a JEOL 2100F transmission electron microscope (TEM/STEM) operating at 200 kV and equipped with a field emission electron gun, providing a point resolution of 0.19 nm; samples were prepared by placing a drop of a dilute toluene or ethanol dispersion of nanoparticles onto a 300 mesh carbon-coated copper grid and evaporated immediately at 60 °C.  $^1\text{H}$  NMR spectra were recorded on a spectrometer Bruker AMX-300 using  $\text{DMSO-d}_6$  as solvent and TMS as internal reference.

## 3. Results and discussion

$\text{TiO}_2$  particles with distinct morphologies have been synthesized under soft, non-aqueous, ethanolic conditions. All reactions were carried out at 78 °C using  $\text{Ti}(\text{ButO})_4$  as the starting reagent.  $\text{Ti}(\text{ButO})_4$  was chosen as Ti precursor for its slow rate of hydrolysis, due to the butoxide group, which slows down the process of diffusion and polymerization compared to other alkyl groups. To obtain  $\text{TiO}_2$  nanoparticles a new synthesis method was developed from the basis of that reported by Dinh et al. [28], with EtOH (96%) providing the water necessary to accelerate the hydrolysis reaction, and oleic acid (OA) and oleylamine (OM) as capping agents. Experiments were run in the absence of surfactants as well as with different ratios of oleic acid and oleylamine. In those experiments involving surfactants, the  $\text{Ti}(\text{OBut})_4$ : surfactant molar ratio was kept constant at 1:10.

### 3.1. Growth in the absence of surfactants

When no surfactant is used,  $\text{TiO}_2$  spheres with homogeneous sizes (2–4  $\mu\text{m}$ ) are obtained (Fig. 3). A more detailed analysis of the surface shows that the particles are in fact aggregates of  $\text{TiO}_2$  nanocrystals with a spherical macrostructure (Fig. 3 (b), (d) and (f)), similar to those described in previous works [21,22,37]. This growth should be ascribed to the synthesis route: at low temperature and due to the limited amount of water from air, the formed  $\text{TiO}_2$  crystals are small, and assemble in Ti microspheres with nanosized pores [20]. The crystallinity of the synthesized samples was examined by powder X-Ray diffraction. As shown in Fig. 4, the precipitate presents a low degree of crystallinity, which might be due to the small size of the

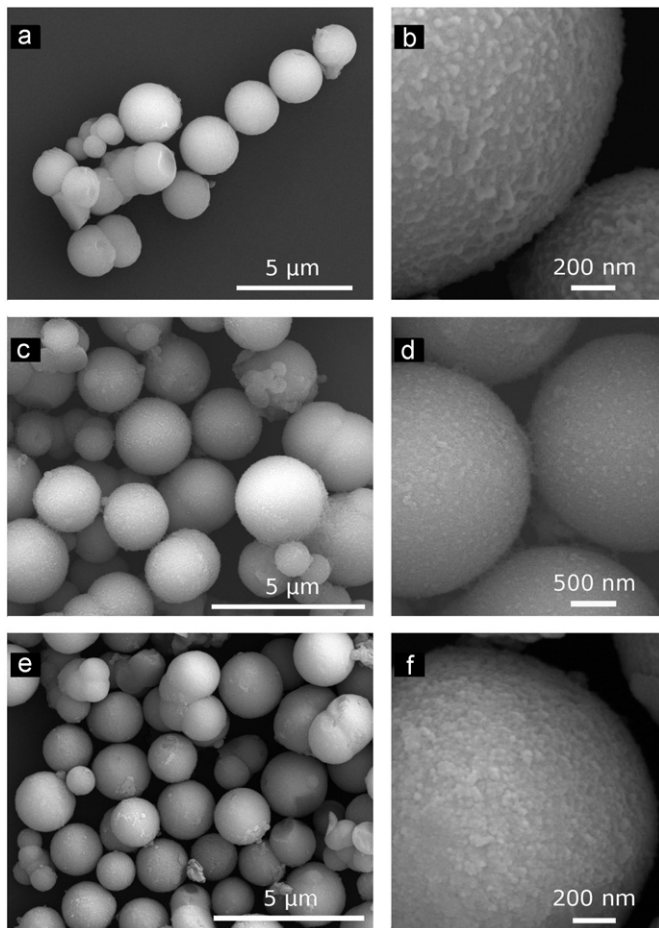


Fig. 3. (a) FESEM micrograph of the sample TiS, (b) detail of the surface of TiS, (c) FESEM micrograph of the sample TiS300, (d) detail of the surface of TiS300, (e) FESEM micrograph of the sample TiS400 and (f) detail of the surface of TiS400.

nanocrystals constituting the spheres ( $\sim 5$  nm). This fact is confirmed in the TEM micrographs (see Fig. 5), whereby the  $\text{TiO}_2$  spheres, formed by small nanocrystals, show a cloud-like appearance. In order to improve the crystallinity of the obtained particles these samples were fired at temperatures of  $300^\circ\text{C}$  (TiS300 samples) and  $400^\circ\text{C}$  (TiS400 samples) for 4 h. As it can be seen in Fig. 4, the degree of crystallinity increases after calcination, due to a growth and consolidation of the nanoparticles (Fig. 3). In both cases crystallization of pure anatase phase (JCPDS File no. 21-1272) is observed, and FESEM micrographs confirm that the size and macrostructure of the spheres are maintained after calcination (Fig. 3). Therefore, this method of synthesis allows us to obtain crystalline  $\text{TiO}_2$  spheres with homogeneity of sizes and shapes, similar to those described by other authors, but employing mild reaction conditions.

### 3.2. Effect of surfactants and surfactants ratio

The situation significantly changes when the reactions are carried out in the presence of oleylamine and oleic acid,

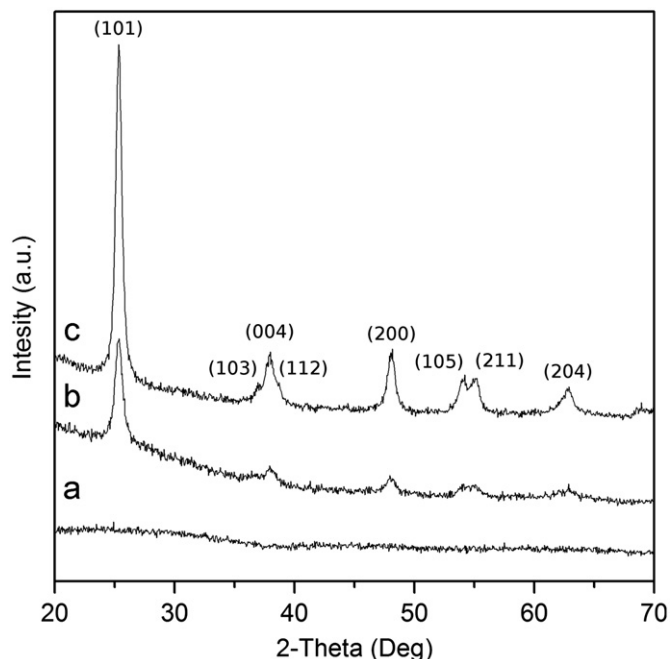


Fig. 4. XRD diffraction patterns of the TiS samples: (a) TiS, (b) TiS300 and (c) TiS400.

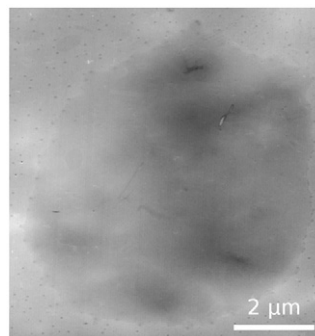


Fig. 5. Low-magnification TEM micrograph of an individual sphere of the sample TiS.

since now faceted nanoparticles of  $\text{TiO}_2$  are obtained. More specifically, when the OA/OM ratio is 5:5 (TiNP5 samples), truncated rhombic-shaped  $\text{TiO}_2$  nanoparticles are obtained, with a size of about 25 nm (Fig. 6(a)). A modification of the surfactants ratio to 6:4 (TiNP6 samples) leads to the formation of  $\text{TiO}_2$  nanoparticles with similar size and morphology, together with the formation of  $\text{TiO}_2$  nanorods (Fig. 6(b)). The crystallinity of the synthesized samples was verified by selected area electron diffraction (SAED) (Fig. 6(c)). This change in the growth habit with regard to the surfactant-free compositions must be interpreted as follows: as mentioned in the introduction, the shape of the final products is affected by the rate of the two main processes which control the formation of  $\text{TiO}_2$ , i.e. hydrolysis of the titanium precursor and the subsequent condensation reactions to form a Ti–O–Ti network [38]. By using surfactants with different functional groups and distinct binding strengths, the morphology of resulting

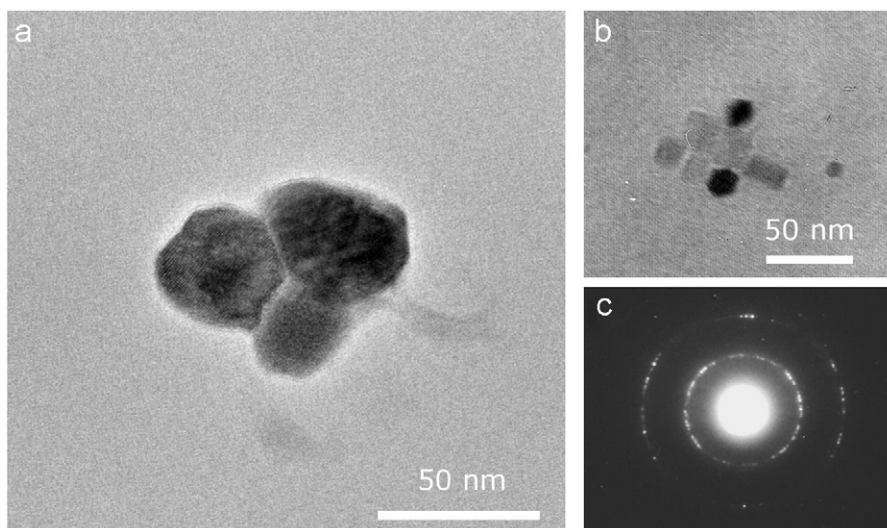


Fig. 6. Representative TEM images of: (a) TiNP5 obtained at 78 °C for 8 h, (b) TiNP6 obtained at 78 °C for 8 h and (c) SAED of truncated rhombic TiO<sub>2</sub> nanoparticles.

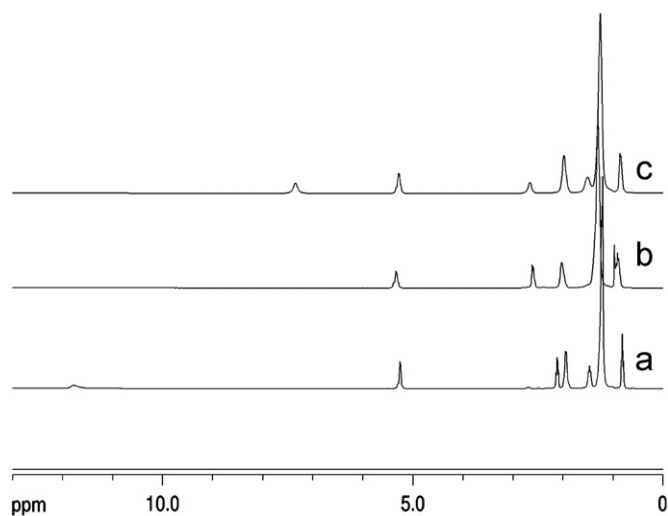


Fig. 7. <sup>1</sup>H NMR spectra in DMSO-d<sub>6</sub> of: (a) oleic acid (OA), (b) oleylamine (OM) and (c) dioleamide (DO).

particles could be controlled [39–41]. In our case it has been suggested that OA strongly binds to the TiO<sub>2</sub> {001} faces [25,28], whereas OM tends to adhere on the {101} ones [18]. Thus, varying the proportions of these compounds it is possible to modulate the rate of hydrolysis and promote the formation of TiO<sub>2</sub> nanoparticles with controlled shape and size [28]. Nevertheless, there is still a fact that must be considered: oleylamine and oleic acid condense exothermically in situ to form a long-chain amide, dioleamide (DO) [42], in a visible spontaneous process, which is confirmed by <sup>1</sup>H NMR spectroscopy. As shown in Fig. 7, after condensation the spectrum of the obtained product (DO) shows a new signal at 7.35 ppm, which corresponds to the H<sub>c</sub> and NH group. Furthermore, the lack of any signal above 10 ppm confirms the loss of the hydrogen belonging to the carboxylic group. Finally, some signals are shifted compared to the free precursors. These

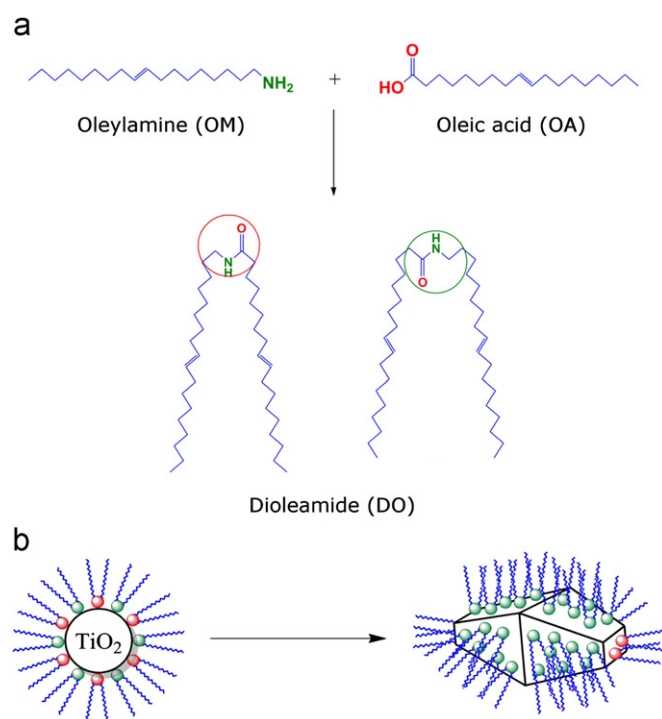


Fig. 8. (a) Oleic acid (OA) and oleylamine (OM) condensation and (b) shape control of dioleamide (DO) depending of the bond selectivity and strength.

facts confirm that the formation of DO was near completion after the addition of both compounds. This new formed molecule also plays a role as a surfactant [43], and according to our results it may also bind onto the TiO<sub>2</sub> faces with different strengths: more selectively to the {001} and {010} faces through the –C=O group and in a weaker way to the {101} faces through the –NH group (Fig. 8). These selective bindings of the DO molecule to different facets of the TiO<sub>2</sub> crystals restrict growth in the corresponding directions, as we have observed. On the

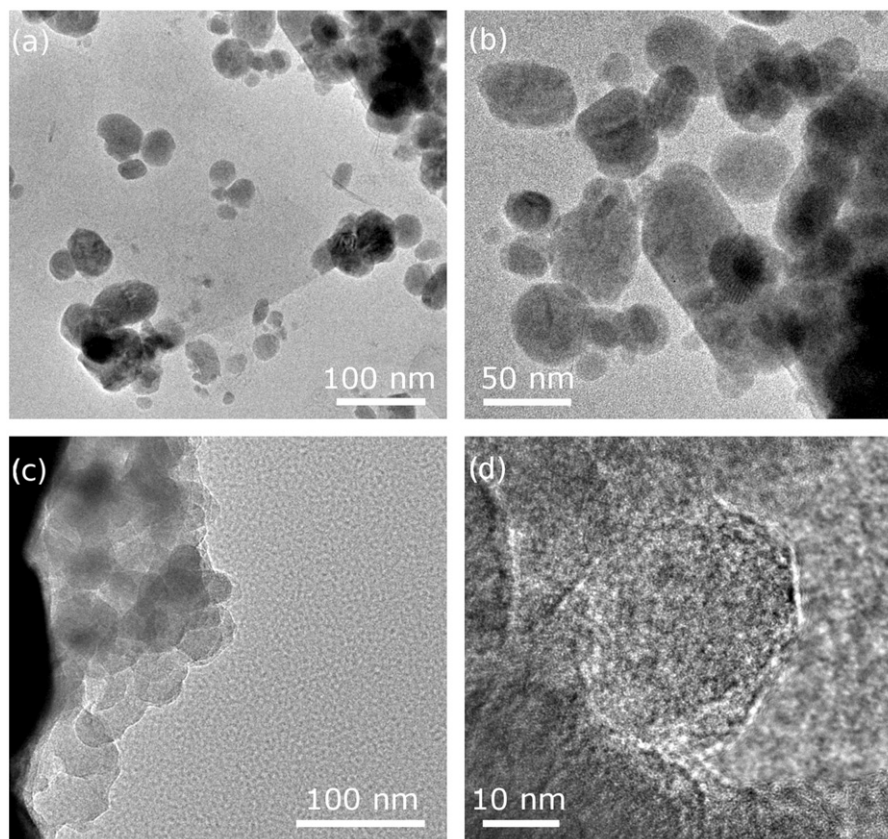


Fig. 9. TEM images of: (a) and (b) TiNP5 obtained at 78 °C for 72 h, (c) TiNP6 and (d) an individual particle of TiNP6 obtained at 78 °C for 72 h.

other hand, when the OA/OM mole ratio is changed to 6:4 (TiNP6 samples), there is an excess of unreacted OA and therefore an equilibrium is set between the binding of DO and OA to  $\{001\}$  faces. Due to the higher electronegativity of the carboxylic group belonging to OA, this probably binds more strongly and selectively to  $\{001\}$  faces, and as a result both  $\text{TiO}_2$  truncated nanooctahedrons and  $\text{TiO}_2$  nanorods are promoted.

### 3.3. Effect of reaction time

In order to evaluate how reaction time affects morphology of the particles, the reactions with 5:5 and 6:4 surfactants ratios were carried out, increasing the time up to 72 h ( $T=78\text{ °C}$ ). As it can be observed in Fig. 9, the truncated rhombic nanoparticles retain their morphology, but no nanorods are observed this time. Once more crystallinity of the particles was verified by SAED (not depicted here). In the particular case of samples with 5:5 OA/OM molar ratio, merely an increase in the average particle size ( $> 50\text{ nm}$ ) is produced. However, in samples with 6:4 OA/OM molar ratio significant changes have been generated: the truncated octahedrons have been elongated in the  $[001]$  direction and this is due to the developing of new  $\{010\}$  facets (Fig. 9(c) and (d)). This situation can be ascribed to a kinetic regime [44], i.e. to the fact that the crystals grow faster on the faces with higher surface energy:  $\{001\}$  and  $\{010\}$ . Actually, our experiments with

6:4 OA/OM molar ratio (TiNP6 samples) suggest that the growth of the  $\{001\}$  faces is initially faster than that of the  $\{010\}$  ones, but beyond a certain point which we achieve by increasing the reaction time, the preferential growth switches to the  $\{010\}$  faces. Furthermore, Barnard et al. [45] also found that the formation of these new  $\{010\}$  facets is encouraged by conditions in which oxygenated surfaces are favored, something that we have in the TiNP6 samples with a higher amount of OA (6:4 M ratio) in the reaction medium.

## 4. Conclusions

A sustainable and versatile synthesis method has been developed which allows to obtain morphologically-tailored  $\text{TiO}_2$  nanoparticles at extraordinarily soft solution conditions. Anatase nanostructured hierarchical spheres as well as individual nanoparticles with exposed high-energy facets ( $\{001\}$  and  $\{010\}$ ) can be obtained at atmospheric pressure and temperatures as low as 78 °C. The strategy is based on the use of a non-aqueous alcoholic reaction medium with water traces to accelerate the hydrolysis of the Ti precursor. These water traces are incorporated either from the air (atmospheric water) or from the ethanol–water azeotropic mixture (ethanol 96%). Besides, organic surfactants based on a combination of oleic acid, oleylamine and the in situ formed dioleamide, have been employed to cap the growth in one or more crystal faces. Consequently the

particles develop only in certain directions, and hence tailoring their morphology. The absence of fluorine-based compounds, which are typically used as capping agents to control the morphology of the growing TiO<sub>2</sub> particles, makes the method here proposed a promising environmental-friendly alternative to current synthesis routes.

## Acknowledgments

This work was supported by the Spanish Ministry of Science and Innovation (MICINN) through the projects IPT-120000-2010-033 (GESHTOS), IPT-2011-1113-310000 (NANOBACK) and CICYTMAT 2010-16614. The Spanish National Research Council (CSIC) and European Science Foundation (ESF) are also acknowledged for a *JAE-Doc* contract to Dr. Teresa Jardiel.

## References

- [1] S. Liu, J. Yu, M. Jaroniec, Anatase TiO<sub>2</sub> with dominant high-energy {001} facets: synthesis, properties, and applications, *Chemistry of Materials* 23 (2011) 4085–4093.
- [2] A. Hegazy, E. Prouzet, Room temperature synthesis and thermal evolution of porous nanocrystalline TiO<sub>2</sub> anatase, *Chemistry of Materials* 24 (2012) 245–254.
- [3] J.J. Wu, X.J. Lü, L.L. Zhang, F.Q. Huang, F.F. Xu, Dielectric constant controlled solvothermal synthesis of a TiO<sub>2</sub> photocatalyst with tunable crystallinity: a strategy for solvent selection, *European Journal of Inorganic Chemistry* 19 (2009) 2789–2795.
- [4] M. Li, Z.L. Hong, Y.N. Fang, F.Q. Huang, Synergistic effect of two surface complexes in enhancing visible-light photocatalytic activity of titanium dioxide, *Materials Research Bulletin* 43 (2008) 2179–2186.
- [5] X.J. Lü, X. Mou, J.J. Wu, D.W. Zhang, L.L. Zhang, F.Q. Huang, F.F. Xu, S.M. Huang, Improved-performance dye-sensitized solar cells using Nb-doped TiO<sub>2</sub> electrodes: efficient electron injection and transfer, *Advanced Functional Materials* 20 (2010) 509–515.
- [6] M. Grätzel, Photochemical cells, *Nature* 414 (2001) 338–344.
- [7] X. Chen, S.S. Mao, Titanium dioxide nanomaterials: synthesis, properties, modifications, and applications, *Chemical Reviews* 107 (2007) 2891–2959.
- [8] E.A. Rozhkova, I. Ulasov, B. Lai, N.M. Dimitrijevic, M.S. Lesniak, T. Rajh, A high-performance nanobio photocatalyst for targeted brain cancer therapy, *Nano Letters* 9 (2009) 3337–3342.
- [9] D. Wang, D. Choi, J. Li, Z. Yang, Z. Nie, R. Kou, D. Hu, C. Wang, L.V. Saraf, J. Zhang, I.A. Aksay, J. Liu, Self-assembled TiO<sub>2</sub>-graphene hybrid nanostructures for enhanced Li-ion insertion, *ACS Nano* 3 (2009) 907–914.
- [10] X.J. Lü, F.Q. Huang, X.L. Mou, Y.M. Wang, F.F. Xu, A general preparation strategy for hybrid TiO<sub>2</sub> hierarchical spheres and their enhanced solar energy utilization efficiency, *Advanced Materials* 22 (2010) 3719–3722.
- [11] D. Kim, A. Ghicov, S.P. Albu, P.J. Schmuki, Bamboo-type TiO<sub>2</sub> nanotubes: improved conversion efficiency in dye-sensitized solar cells, *Journal of the American Chemical Society* 130 (2008) 16454–16455.
- [12] S.W. Kim, T.H. Han, J. Kim, H. Gwon, H.S. Moon, S.W. Kang, S.O. Kim, K. Kang, Fabrication and electrochemical characterization of TiO<sub>2</sub> three-dimensional nanonetwork based on peptide assembly, *ACS Nano* 3 (2009) 1085–1090.
- [13] S. Joo, I. Muto, N. Hara, Hydrogen gas sensor using Pt- and Pd-added anodic TiO<sub>2</sub> nanotube films, *Journal of the Electrochemical Society* 157 (2010) J221–J226.
- [14] H.G. Yang, C.H. Sun, S.Z. Qiao, J. Zou, G. Liu, S.C. Smith, H.M. Cheng, G.Q. Lu, Anatase TiO<sub>2</sub> single crystals with a large percentage of reactive facets, *Nature* 453 (2008) 638–641.
- [15] H. Yang, G. Liu, S. Qiao, C. Sun, Y. Jin, S.C. Smith, J. Zou, H.M. Cheng, G.Q. Lu, Solvothermal synthesis and photoreactivity of anatase TiO<sub>2</sub> nanosheets with dominant {001} facets, *Journal of the American Chemical Society* 131 (2009) 4078–4083.
- [16] X. Han, Q. Kuang, M. Jin, Z. Xie, L. Zheng, Synthesis of titania nanosheets with a high percentage of exposed (001) facets and related photocatalytic properties, *Journal of the American Chemical Society* 131 (2009) 3152–3153.
- [17] Y. Dai, C.M. Cobley, J. Zeng, Y. Sun, Y. Xia, Synthesis of anatase TiO<sub>2</sub> nanocrystals with exposed {001} facets, *Nano Letters* 9 (2009) 2455–2459.
- [18] J. Joo, S.G. Kwon, T. Yu, M. Cho, J. Lee, J. Yoon, T. Hyeon, Large-scale synthesis of TiO<sub>2</sub> nanorods via nonhydrolytic sol-gel ester elimination reaction and their application to photocatalytic inactivation of *E. coli*, *Journal of Physical Chemistry B* 109 (2005) 15297–15302.
- [19] J. Li, L.W. Wang, Shape effects on electronic states of nanocrystals, *Nano Letters* 3 (2003) 1357–1363.
- [20] X. Lü, S. Ding, Y. Xie, F. Huang, Non-aqueous preparation of high-crystallinity hierarchical TiO<sub>2</sub> hollow spheres with excellent photocatalytic efficiency, *European Journal of Inorganic Chemistry* (2011) 2879–2883.
- [21] Z. Zheng, B. Huang, X. Qin, X. Zhang, Y. Dai, M. Jiang, P. Wang, M.H. Whangbo, Highly efficient photocatalyst: TiO<sub>2</sub> microspheres produced from TiO<sub>2</sub> nanosheets with a high percentage of reactive {001} facets, *Chemistry—A European Journal* 15 (2009) 12576–12579.
- [22] Z. Zheng, B. Huang, J. Lu, X. Qin, X. Zhang, Y. Dai, Hierarchical TiO<sub>2</sub> microspheres: synergetic effect of {001} and {101} facets for enhanced photocatalytic activity, *Chemistry—A European Journal* 17 (2011) 15032–15038.
- [23] J.N. Hay, H.M. Raval, Synthesis of organic-inorganic hybrids via the non-hydrolytic sol-gel process, *Chemistry of Materials* 13 (2001) 3396–3403.
- [24] M. Niederberger, M.H. Bartl, G.D. Stucky, Benzyl alcohol and transition metal chlorides as a versatile reaction system for the nonaqueous and low-temperature synthesis of crystalline nano-objects with controlled dimensionality, *Journal of the American Chemical Society* 124 (2002) 13642–13643.
- [25] Y.W. Jun, M.F. Casula, J.H. Sim, S.Y. Kim, J. Cheon, A.P. Alivisatos, Surfactant-assisted elimination of a high energy facet as a means of controlling the shapes of TiO<sub>2</sub> nanocrystals, *Journal of the American Chemical Society* 125 (2003) 15981–15985.
- [26] Z. Zhang, X. Zhong, S. Liu, D. Li, M. Han, Aminolysis route to monodisperse titania nanorods with tunable aspect ratio, *Angewandte Chemie International Edition* 44 (2005) 3466–3470.
- [27] R. Buonsanti, V. Grillo, E. Carlino, C. Giannini, T. Kipp, T.R. Cingolani, D. Cozzoli, Nonhydrolytic synthesis of high quality anisotropically shaped brookite TiO<sub>2</sub> nanocrystals, *Journal of the American Chemical Society* 130 (2008) 11223–11233.
- [28] C.T. Dinh, T.D. Nguyen, F. Kleitz, T.O. Do, Shape-controlled synthesis of highly crystalline titania nanocrystals, *ACS Nano* 3 (2009) 3737–3743.
- [29] M. Peiteado, T. Jardiel, F. Rubio, A.C. Caballero, Multipod structures of ZnO hydrothermally grown in the presence of Zn<sub>3</sub>P<sub>2</sub>, *Materials Research Bulletin* 45 (2010) 1586–1592.
- [30] H.G. Yang, C.H. Sun, S.Z. Qiao, J. Zou, G. Liu, S.C. Smith, H.M. Cheng, G.Q. Lu, Anatase TiO<sub>2</sub> single crystals with a large percentage of reactive facets, *Nature* 453 (2008) 638–641.
- [31] J. Pan, G. Liu, G.Q.M. Lu, H.M. Cheng, On the true photoreactivity order of {001}, {010}, and {101} facets of anatase TiO<sub>2</sub> crystals, *Angewandte Chemie International Edition* 50 (2011) 2133–2137.
- [32] X.H. Yang, Z. Li, C. Sun, H.G. Yang, C. Li, Hydrothermal stability of {001} faceted anatase TiO<sub>2</sub>, *Chemistry of Materials* 23 (2011) 3486–3494.

- [33] C.Z. Wen, H.B. Jiang, S.Z. Qiao, H.G. Yang, G.Q. Lu, Synthesis of high-reactive facets dominated anatase TiO<sub>2</sub>, *Journal of Materials Chemistry* 21 (2011) 7052–7061.
- [34] Y. Yin, A.P. Alivisatos, Colloidal nanocrystals synthesis and the organic–inorganic interface, *Nature* 437 (2005) 664–670.
- [35] S.G. Kwon, T. Hyeon, Colloidal chemical synthesis and formation kinetics of uniformly sized nanocrystals of metals, oxides, and chalcogenides, *Accounts of Chemical Research* 41 (2008) 1696–1709.
- [36] X. Wang, Q. Peng, Y. Li, Interface-mediated growth of monodispersed nanostructures, *Accounts of Chemical Research* 40 (2007) 635–643.
- [37] J.S. Chen, Y.L. Tan, C.M. Li, Y.L. Cheah, D. Luan, S. Madhavi, F.Y.C. Boey, L.A. Archer, X.W. Lou, Constructing hierarchical spheres from large ultrathin anatase TiO<sub>2</sub> nanosheets with nearly 100% exposed (001) facets for fast reversible lithium storage, *Journal of the American Chemical Society* 132 (2010) 6124–6130.
- [38] J. Livage, M. Henry, C. Sanchez, Sol–gel chemistry of transition metal oxides, *Progress in Solid State Chemistry* 18 (1988) 259–341.
- [39] E. Ramirez, S. Jansat, K. Philippot, P. Lecante, M. Gomez, A.M. Masdeu-Bulto, B. Chaudret, Influence of organic ligands on the stabilization of palladium nanoparticles, *Journal of Organometallic Chemistry* 689 (2004) 4601–4610.
- [40] H.X. Mai, Y.W. Zhang, R. Si, Z.G. Yan, L.D. Sun, L.P. You, C.H. Yan, High-quality sodium rare-earth fluoride nanocrystals: controlled synthesis and optical properties, *Journal of the American Chemical Society* 128 (2006) 6426–6436.
- [41] J. Watt, N. Young, S. Haigh, A. Kirkland, R.D. Tilley, Synthesis and structural characterization of branched palladium nanostructures, *Advanced Materials* 21 (2009) 2288–2293.
- [42] B.D. Fahlman, Nanoscale building blocks and applications, in: *Materials Chemistry*, 2nd ed., Springer-Verlag New York LLC, New York, 2008, pp. 517–518.
- [43] H. Wu, Y. Yang, Y.C. Cao, Synthesis of colloidal uranium-dioxide nanocrystals, *Journal of the American Chemical Society* 128 (2006) 16522–16523.
- [44] Y.W. Jun, Y.Y. Jun, J.J. Cheon, Architectural control of magnetic semiconductor nanocrystals, *Journal of the American Chemical Society* 124 (2001) 615–619.
- [45] A.S. Barnard, L.A. Curtiss, Prediction of TiO<sub>2</sub> nanoparticle phase and shape transitions controlled by surface chemistry, *Nano Letters* 5 (2005) 1261–1266.